nature COMMUNICATIONS

ARTICLE

Received 15 Jul 2013 | Accepted 4 Nov 2013 | Published 9 Dec 2013

DOI: 10.1038/ncomms3861

Supramolecular high-aspect ratio assemblies with strong antifungal activity

Kazuki Fukushima[1,2,*], Shaoqiong Liu[3,*], Hong Wu[3], Amanda C. Engler[1], Daniel J. Coady[1], Hareem Maune[1], Jed Pitera[1], Alshakim Nelson[1], Nikken Wiradharma[3], Shrinivas Venkataraman[3], Yuan Huang[4], Weimin Fan[4], Jackie Y. Ying[3], Yi Yan Yang[3] & James L. Hedrick[1]

Efficient and pathogen-specific antifungal agents are required to mitigate drug resistance problems. Here we present cationic small molecules that exhibit excellent microbial selectivity with minimal host toxicity. Unlike typical cationic polymers possessing molecular weight distributions, these compounds have an absolute molecular weight aiding in isolation and characterization. However, their specific molecular recognition motif (terephthalamide-bisurea) facilitates spontaneous supramolecular self-assembly manifesting in several polymer-like properties. Computational modelling of the terephthalamide-bisurea structures predicts zig-zag or bent arrangements where distal benzyl urea groups stabilize the high-aspect ratio aqueous supramolecular assemblies. These nanostructures are confirmed by transmission electron microscopy and atomic force microscopy. Antifungal activity against drug-sensitive and drug-resistant strains with *in vitro* and *in vivo* biocompatibility is observed. Additionally, despite repeated sub-lethal exposures, drug resistance is not induced. Comparison with clinically used amphotericin B shows similar antifungal behaviour without any significant toxicity in a *C. albicans* biofilm-induced mouse keratitis model.

[1] IBM Almaden Research Center, 650 Harry Road, San Jose, California 95120, USA. [2] Department of Polymer Science and Engineering, Yamagata University, Yonezawa, Yamagata 992-8510, Japan. [3] Institute of Bioengineering and Nanotechnology, 31 Biopolis Way, The Nanos, Singapore 138669, Singapore. [4] State Key Laboratory for Diagnosis and Treatment of Infectious Diseases, First Affiliated Hospital, College of Medicine, Zhejiang University, Hangzhou 310003, China. * These authors contributed equally to this work. Correspondence and requests for materials should be addressed to Y.Y.Y. (email: yyyang@ibn.a-star.edu.sg) or to J.L.H. (email: hedrick@us.ibm.com).

The number of opportunistic fungal infection cases is increasing due to growing populations of immunocompromised patients[1]. These invasive infections are mainly caused by *Candida* and *Aspergillus* species as well as *Cryptococcus neoformans* (*C. neoformans*). It has been reported that candidiasis, a fungal infection caused by *Candida*, was the third most common blood stream infection in the United States[2,3]. Fungal infections resistant to conventional antifungal drugs have been increasingly documented[4,5], and many existing antifungal agents (for example, triazoles and polyenes) have witnessed resistance development in patients[1]. This is of huge concern within health-care and clinical settings due to the extremely limited selection of antifungal agents.

Another challenge in developing antifungal drugs is that fungi are metabolically similar to mammalian cells, providing limited fungi-specific targets. For example, amphotericin B has broad-spectrum antimicrobial activities by binding ergosterol, the key sterol in fungal membrane, to form aggregates[6]. These aggregates induce membrane pores resulting in cell lysis. In a similar fashion, amphotericin B can also bind cholesterol in mammalian cell membranes, leading to non-specific toxicity. Haemolysis and nephrotoxicity are commonly reported side-effects caused by this drug in patients[7]. In aggregate, all these issues have created a pressing need for the development of novel antifungal agents that are efficient and pathogen-specific.

Host defence peptides and synthetic polymers are two classes of macromolecules currently being studied as effective antimicrobials[8–11]. These materials are amphiphilic while also carrying cationic charge. They selectively interact and disintegrate negatively charged microbial walls or membranes via electrostatic interactions and insertion into membrane lipid domains. In addition, it is difficult for microbial cells to repair a physically damaged cell wall or membrane, hence avoiding potential microbial resistance development. Despite their efficacious antimicrobial activity, both peptides and synthetic polymers have seen limited clinical applications because of several inherent problems. For example, antimicrobial peptides generally have a short half-life *in vivo* due to enzymatic degradation, and suffer from high production costs. Bio-inspired synthetic polymers have been reported and have achieved considerable success in overcoming some of the drawbacks found with antimicrobial peptides, but many of them are cytotoxic to mammalian cells.

In this study, we describe the synthesis, self-assembly and therapeutic activity for a novel class of discrete low-molecular weight antifungal agents. Their chemical structures are designed to incorporate specific molecular recognition motifs that induce formation of high-aspect ratio supramolecular assemblies. The assembled structures have polymer-like properties including a glass transition temperature (T_g), and fibre-like morphologies in water. Compared with discrete molecules, fibre formation increases local concentration of cationic charges and compound mass, which facilitates the targeting and subsequent fungal membrane lysis with high efficiency and minimal haemolysis/cytotoxicity at concentrations far exceeding the therapeutic dosage. The nano-assemblies are effective against clinically isolated drug-resistant fungi and fungal biofilm, and prevent drug resistance development. In a fungal keratitis mouse model, these nanostructures decrease the severity of keratitis without causing any toxicity.

Results

Compound synthesis and characterization. A key design motif of these small molecules was the rigid terephthalamide diamine that was readily modified to generate cationic terephthalamide-bisurea amphipathic compounds. These monodisperse molecules were constructed in a one-pot synthesis by reaction of a diamine with bis(pentafluorophenyl)carbonate generating reactive carbamates (Fig. 1). Subsequent reaction with an alkyl diamine, where a single amine group was previously protected by *tert*-butyloxycarbonyl (^{t}Boc), generated the terephthalamide-bisurea compound readily isolated by precipitation into ether. These compounds were then dissolved in trifluoroacetic acid (TFA) (20 h) for removal of ^{t}Boc groups and generation of amine/TFA salts, again isolated by simple precipitation in ether. Four compounds were prepared having ethyl, butyl, hexyl and benzyl amine spacers between the urea and cationic charge, with absolute molecular weights ranging from 774.7 to 926.9 g mol^{-1} (Supplementary Figs S1–S4; Supplementary Table S1 and Supplementary Methods).

Interestingly, these compounds did not show a melting point, but rather manifested a T_g as confirmed by both differential scanning calorimetry (DSC) and dynamic mechanical analysis (DMA) performed on a solid support. For example, compound **3b** showed a T_g at ~120 °C (DSC), and an associated modulus drop and tan δ increase via DMA (Fig. 2a,b). These findings indicated similarities to the amorphous glasses synthesized by Ober *et al.*[12], low molecular weight resist compounds that have a T_g, low viscosity and distinctive dissolution properties due to the lack of molecular weight distribution. Furthermore, the aforementioned compounds formed supramolecular structures with cationic surfaces (zeta potential: 32–45 mV) when dissolved in water above their critical micellar concentrations (CMCs) (12-100 mg l^{-1} in de-ionized water; 6–56 mg l^{-1} in the fungus culture medium) (Table 1). For example, **3b** and **3d** formed the nanofibers (several μm and several hundred nm in length, ~5 nm and ~10 nm in diameter, respectively) after dialysis against water, as seen by transmission electron microscopy (TEM) (Fig. 2d,e, respectively). Interestingly, **3b** self-assembled into nanofibers with high flexibility, while **3d** formed relatively rigid nanofibers presumably due to its rigid molecular structure. Solution atomic force microscopy (AFM) of **3b** (Fig. 2c) also shows anisotropic structures, although of considerably shorter lengths. Molecular mechanics conformational analysis of the terephthalamide-bisurea core structure revealed a zig-zag or bent structure with distal benzyl urea groups perpendicular to the terephthalamide core (Fig. 1 and Supplementary Fig. S5). These zig-zag structures pack together into planar sheets stabilized by urea–urea hydrogen bonds and aromatic stacking. As the amide and urea groups are perpendicular, planar sheets further stack against one another, stabilized by hydrophobic interactions and amide–amide hydrogen bonds, generating a multilayer nanorod (Fig. 1 and Supplementary Fig. S5). This cross-braced nanorod structure is mechanically stable and allows high-aspect ratio structures.

***In vitro* antifungal activity**. We evaluated these cationic assemblies for antifungal activity against clinically relevant *C. albicans*, clinically isolated drug-sensitive and drug-resistant *C. neoformans* fungi. The overall net cationic charge of the assemblies allowed sufficient electrostatic interactions with anionic fungal cell surfaces. The compounds **3a**–**3d** inhibited fungal growth at relatively low minimum inhibitory concentration (MIC) values, which were greater than their CMCs in the fungus culture medium (Table 1). In addition, MIC values remained unchanged when the fungal concentration varied from 10^2 to 10^5 CFU ml^{-1} (Supplementary Fig. S6). These findings indicated that the compounds were active as aggregate assemblies rather than discrete molecules. This is particularly important as the cell wall of *C. albicans* consists of multiple layers with low negative charges (zeta potential: −4 mV), which impairs the ability of cationic nanoparticles to

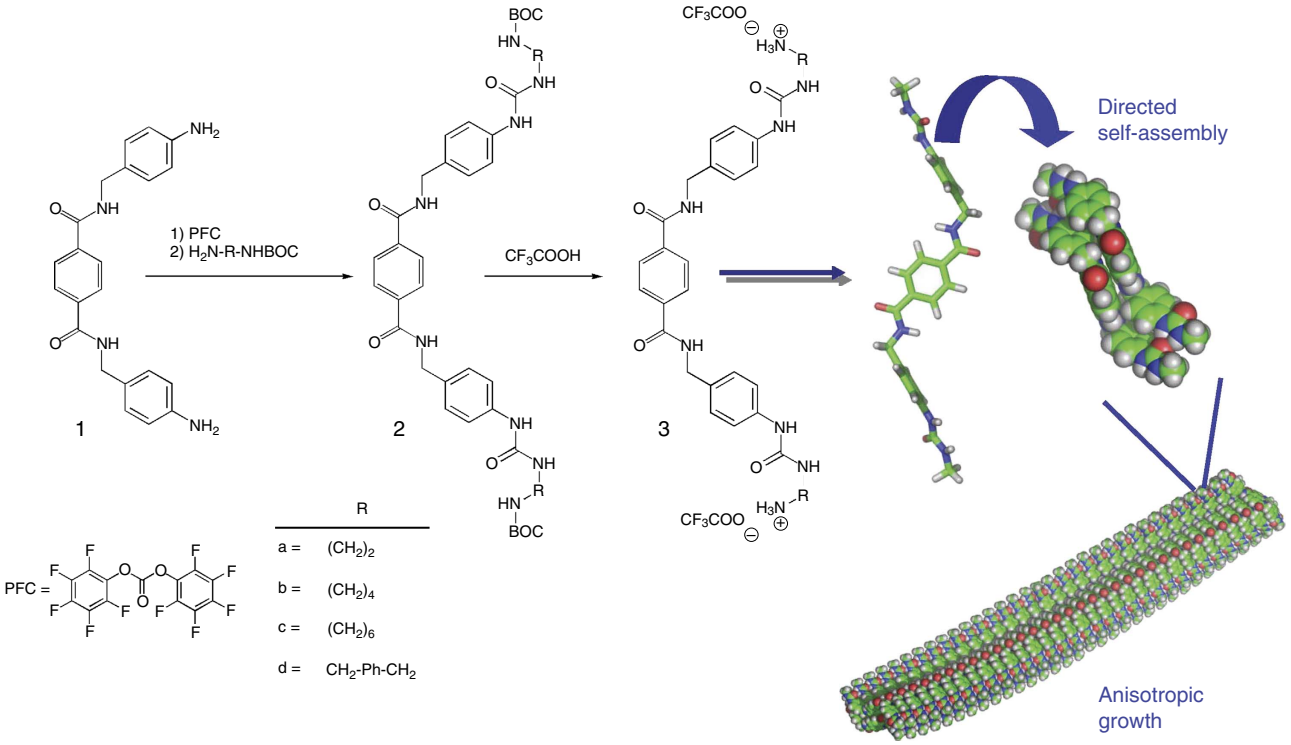

Figure 1 | Synthesis and characteristics of compounds 3a–d. Self-assembly motif with tunable functional groups. Molecular mechanics conformational analysis of the terephthalamide-bisurea structure revealed a zig-zag or bent structure with the distal benzyl urea groups perpendicular to the terephthalamide nanorod structure that is mechanically stable and is capable of generating high aspect structures.

adhere to the cell wall and cause membrane disruption and lysis. The antifungal activity might be attributed to the nanostructure formation (Fig. 2c), facilitating cell wall/membrane penetration. Additionally, increasing hydrophobicity of the terminal groups from $(CH_2)_2$ (**3a**) to $(CH_2)_4$ (**3b**) improved antifungal efficacy (Fig. 1). However, further increasing the hydrophobicity from $(CH_2)_4$ to $(CH_2)_6$ (**3c**) did not affect antifungal activity. The compound **3d** that can form rigid nanofibers had higher efficacy against *C. neoformans* as compared with **3a**–**3c**. In order to determine microbicidal properties, colony assays were performed. Fluconazole demonstrated fungistatic characteristic against *C. albicans* (MIC: $2\,mg\,l^{-1}$) (Fig. 3a) and *C. neoformans* (MIC: $8\,mg\,l^{-1}$) (Fig. 3b) even at $2\times$ MIC. At these concentrations, the reduction in the viable colony counts of fungi after treatment with fluconazole was <3 log_{10} as compared with the control without the treatment. This phenomenon was also reported by others[13]. However, *C. albicans* and *C. neoformans* treated with the assemblies for 24 h showed >3 log_{10} reduction in the viable colony counts as compared with the control group (that is, $>99.9\%$ eradication) using concentrations at their MIC (Fig. 3a,b), and they were almost completely killed ($\sim100\%$) at $2\times$ MIC, indicating a fungicidal mechanism. The capability of cationic compounds for killing fungi was further investigated by analysing the viable colony counts of *C. albicans* upon treatment at MIC concentration utilizing various exposure times. Notably, $>80\%$ of *C. albicans* cells exposed to **3b** were killed at 30 min, and $>99.9\%$ eradication was found at 1 h (Supplementary Fig. S7).

The antifungal effect of **3a** and **3b** was further investigated against clinically isolated fluconazole-resistant *C. neoformans*. MIC of fluconazole against this strain of fungus increased from 2 (against drug-sensitive strain) to $62.5\,mg\,l^{-1}$, verifying that this strain of fungus was resistant to fluconazole[14]. The MICs of **3a** and **3b** were 125.0 and $62.5\,mg\,l^{-1}$, respectively, which were the same as those against drug-sensitive *C. neoformans*. At and above their MICs, both cationic assemblies removed almost 100% fluconazole-resistant *C. neoformans* cells, while fluconazole was fungistatic as expected (reduction in the viable colony counts of fungi after fluconazole treatment: <3 log_{10} as compared with the control without the treatment) (Fig. 3c). These results indicated that **3a** and **3b** were effective against both drug-sensitive and drug-resistant fungi. Furthermore, multiple sub-lethal dose treatments of *C. albicans* with cationic assemblies did not induce resistance. In contrast, drug resistance was developed after six sub-lethal fluconazole exposures (Fig. 3d). In addition, the cationic assemblies were fungicidal at MIC with $>99.9\%$ killing efficiency of *C. albicans* at passages 1–11, while fluconazole was fungistatic towards *C. albicans* even at $62.5\times$ MICs (Supplementary Fig. S8). These findings demonstrated great potential of the cationic assemblies against drug resistance.

Biofilm lysis. Medical implants beset by fungal biofilm formations, especially those that are resistant to clinical antifungal agents such as amphotericin B and fluconazole[15,16], are a major cause for device failures. To evaluate biofilm disruption ability, cationic assembly **3b** was utilized for the treatment of contact lenses having a *C. albicans* biofilm in order to mimic fungal keratitis *in vitro*[17]. The untreated biofilm consisted of both metabolically active oval and long tubular hyphae cell types (red region), where extracellular matrix (ECM) (green region) was bound in both of them (Fig. 4a,c). In contrast, **3b** treatment mediated a significant reduction in the metabolically active cells (Fig. 4d), and cell wall/membrane of *C. albicans* was broken and debris was observed after the treatment (Fig. 4b). XTT and Safranin assays further confirmed the drastic decrease in *C. albicans* survival and the biofilm disruption after **3b** treatment (Supplementary Fig. S9).

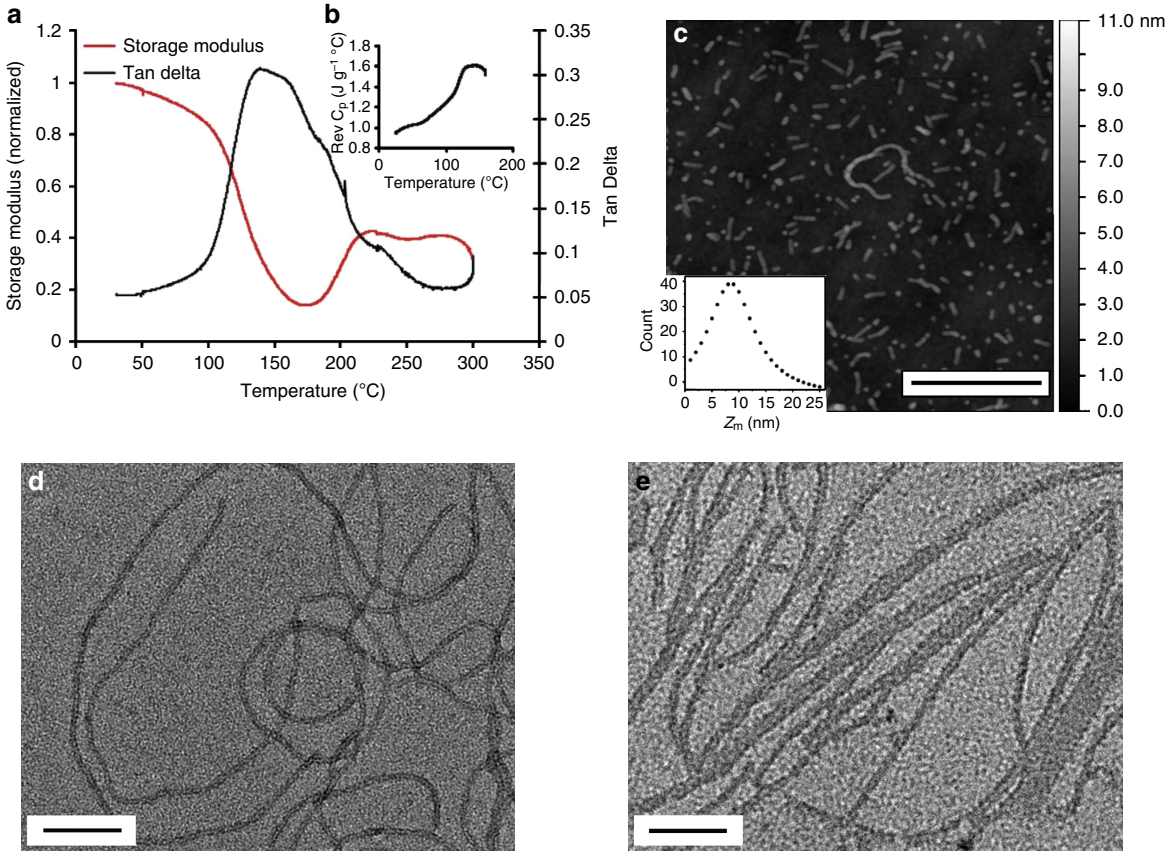

Figure 2 | Polymer-like properties. (**a**) DMA and (**b**) DSC thermograms of compound **3a**. (**c**) Topography micrograph of supramolecular assemblies of **3b** using AFM in fluid. Sample was prepared by direct dissolution of compound **3b** in water and imaged under water. The inset shows a distribution of statistical mean height (z_m) obtained through particle analysis. A Lorentzian fit to the distribution gives a z_m of ~8 nm in water. Scale bar: 500 nm. TEM micrographs of (**d**) compound **3b** and (**e**) compound **3d**. Scale bar: 100 nm.

Table 1 | Physicochemical and biological properties of the cationic compounds.

Compound	R	CMC* (mg l^{-1})	Zeta Potential (mV)	MIC (mg l^{-1})	
				C. A.	C. N.
3a	$(CH_2)_2$	100.0 (56.0)	32.2	62.5	125.0
3b	$(CH_2)_4$	20.0 (14.0)	36.7	31.2	62.5
3c	$(CH_2)_6$	15.0 (13.0)	35.3	31.2	62.5
3d	CH_2-Ph-CH_2	12.0 (6.0)	45.1	31.2	31.2

C. A., C. albicans; *C. N., C. neoformans*; MIC, minimum inhibitory concentration.
*Measured in DI water with 1,000 mg l^{-1}; the values in parenthesis were measured in yeast mould broth

Antifungal mechanism. The antifungal mechanism was studied by visualizing a typical cell structure (that is *C. neoformans* and *C. albicans*) before and after treatment via scanning electron microscopy (SEM) and TEM. Prior to treatment, all fungi showed smooth cellular exteriors and intact cell wall/membrane (Fig. 4e,g—control). After treatment with **3b,** cell wall and membrane damage was easily visible along with dead microbe remnants (Fig. 4f,h—treated). In particular, the membrane damage led to the release of cytoplast from *C. neoformans* cells (Fig. 4h). Fungal membrane damage was also evaluated by measuring the absorbance (260 nm) of cell culture media, which can be directly correlated with nucleic acid release post-treatment[18]. As shown in Supplementary Fig. S10, following treatment of *C. albicans* with **3b**, a significant amount of nucleic acids was observed in the culture media. Furthermore, nucleic acid release was found to be dose-dependent with elevated concentrations of **3b**, causing amplified membrane damage, thereby inducing more cytoplasmic leakage. We postulated that cationic nanorods exploited an associative mechanism (which required appropriately balanced hydrophobic and hydrophilic regions), whereby antifungal material became integrated within the cellular exterior causing membrane destabilization and lysis. This membrane-lytic antifungal mechanism might be the reason for preventing the development of drug resistance (Fig. 3d).

***In vitro* biocompatibility**. A major side effect caused by many cationic antimicrobial peptides and polymers is haemolysis. Haemolytic evaluations were conducted using rat red blood cells incubated with the compounds at various concentrations (Supplementary Fig. S11a). Negligible haemolytic activity was observed for all samples, even at concentrations well above the MIC (up to 1,000 mg l^{-1}), demonstrating excellent selectivity. To evaluate cytotoxicity towards mammalian cells, human dermal fibroblast viability was analysed via MTT assay after incubation with compounds at various concentrations (15.6–1,000 mg l^{-1}) for 24 h (Supplementary Fig. S11b). More than 83% of cells were viable at all concentrations tested, indicating excellent mammalian cell biocompatibility.

***In vivo* antifungal efficacy**. To evaluate the *in vivo* antifungal activity of cationic compounds, fungal keratitis was established in

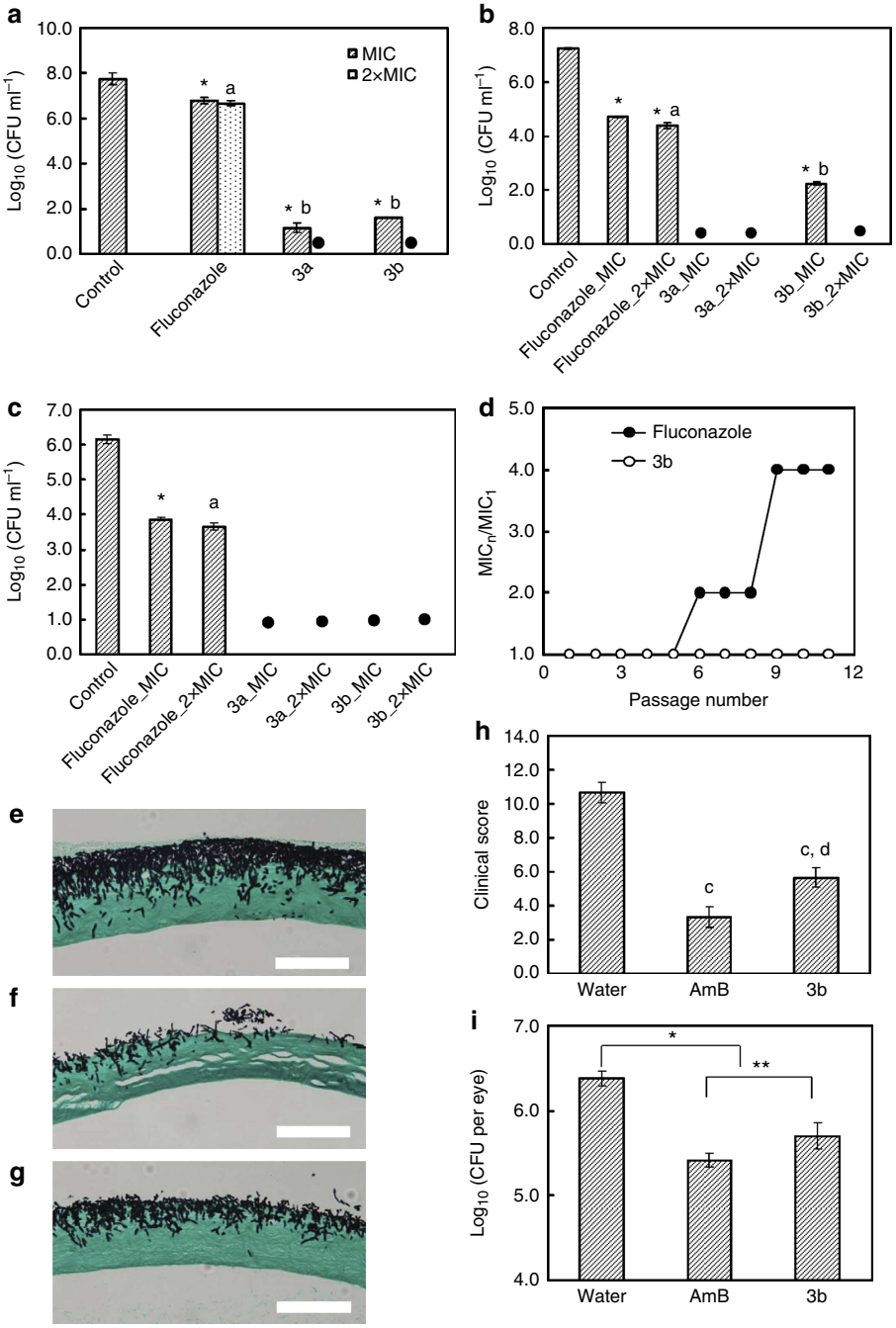

Figure 3 | *In vitro* and *in vivo* antifungal activity. Viable colony counts (Log_{10}) of (**a**) *C. albicans* and (**b**) *C. neoformans* after being treated with **3a**, **3b** and fluconazole at the specified concentrations for 24 h. (**c**) Viable colony counts (Log_{10}) of *C. neoformans* (clinically isolated fluconazole-resistant strain) after treatment with **3a** or **3b** at the specified concentrations for 24 h; fluconazole was used as the control. *$P<0.01$, **3a**, **3b** and fluconazole at their respective MICs versus control; **a**: $P>0.05$, fluconazole at 2 × MIC versus fluconazole at MIC; **b**: $P<0.001$, **3a**, **3b** at MIC versus fluconazole at MIC. Filled black circles indicate that no colony was observed. (**d**) Changes in MICs of antifungal agents upon multiple sub-lethal exposures. (**e**–**g**) Representative histological sections of mouse cornea treated with water (**e**), AmB (**f**) and **3b** (**g**) (Grocott's methenamine silver stain, fungi in black). Scale bar: 100 μm. (**h**) Clinical scores for keratitis after treatment with the topical eye drop solutions. A total score of ≤5, 6–9 and >9 indicate mild, moderate and severe keratitis, respectively. **c**: $P<0.0005$, **3b** and AmB versus control; **d**: $P=0.008$, **3b** versus AmB. (**i**) CFU of *C. albicans* in mouse cornea treated with AmB and **3b**. The data are expressed as mean ± s.d. of 3–6 replicates. *$P<0.01$, **3b** and AmB versus control. **$P>0.05$, **3b** versus AmB.

mice by using contact lens-associated *C. albicans* biofilm infection[19,20]. The experimental protocol was approved by the Institutional Animal Care and Use Committee of Biological Research Centre, Agency for Science, Technology and Research (A*STAR), Singapore. This disease model was chosen because fungal keratitis is a severe eye infection and a major cause of ocular morbidity. An eye ulcer with dense opaque appearance was seen on the eyeballs of the mice with keratitis. The mice were randomly grouped and treated with three topical eye drop solutions: water solution (control), **3b** (2,000 mg l^{-1}) and amphotericin B (AmB) (1,500 mg l^{-1}). AmB was selected as positive control instead of fluconazole because AmB is a

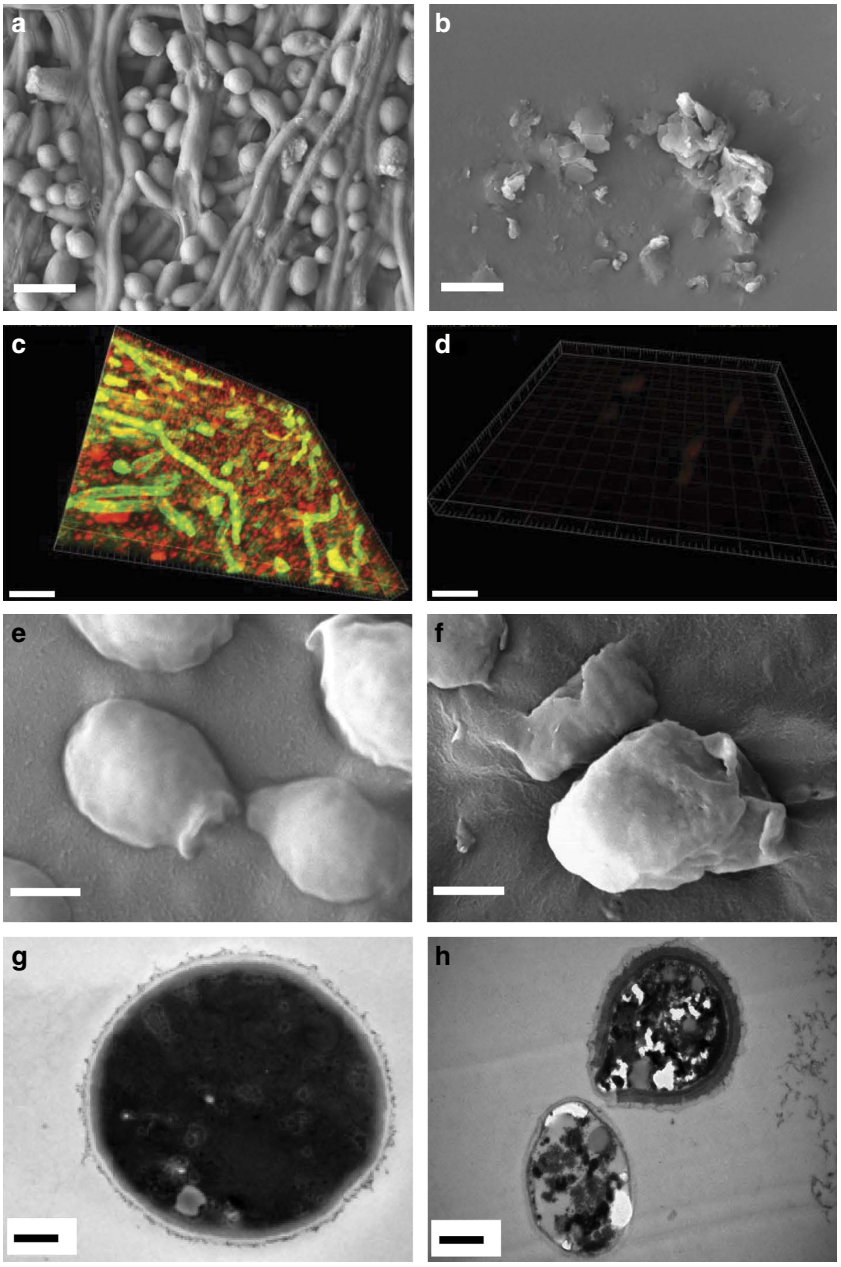

Figure 4 | Biofilm disruption and antifungal mechanism studies. SEM images of *C. albicans* biofilms (**a**) before and (**b**) after treatment with **3b** (scale bar: 5 μm). Confocal images of *C. albicans* biofilms (**c**) before and (**d**) after treatment with **3b** (scale bar: 20 μm). Areas of green fluorescence represents biofilm ECM stained with CON-A, and red fluorescence represents metabolically active cells stained with FUN-1. SEM images of *C. albicans* (**e**) before and (**f**) after treatment with **3b** (scale bar: 1 μm). TEM images of *C. neoformans* (**g**, scale bar: 0.5 μm) before and (**h**, scale bar: 1 μm) after treatment with **3b**.

clinically used strong antifungal agent, while fluconazole was unable to clear *C. albicans* biofilm *in vitro*. In control animals receiving water as eye drops, histological analysis showed extensive hyphal invasion into the corneal stroma (Fig. 3e). In contrast, treatments with **3b** and AmB resulted in significant reduction in the hyphal invasion (Fig. 3f,g and Supplementary Fig. S12), although AmB was relatively more potent. The maximal depth of fungal invasion in the cornea treated with AmB and **3b** was remarkably reduced as compared with that in the control group (18.0 ± 2.1 and 27.6 ± 1.5 μm versus 63.4 ± 5.6 μm) (Supplementary Fig. S12). Keratitis in the control, AmB- and **3b**-treated groups was further evaluated to provide clinical scores of 10.7 ± 0.6, 3.3 ± 0.6 and 5.7 ± 0.6, respectively (Fig. 3h and Supplementary Fig. S13), demonstrating that AmB and **3b** treatment significantly lessened the severity of keratitis ($P < 0.0005$). Importantly, **3b** treatment reduced the number of viable fungi remaining on the eyeballs (measured in colony-forming unit (CFU)) (5.79 $\log_{10}$ CFU per eye versus 6.38 $\log_{10}$ CFU per eye for control, 74.3% reduction, $P < 0.01$) as effectively as AmB (5.44 $\log_{10}$ CFU per eye, 88.7% reduction, $P > 0.05$ as compared with **3b** treatment) (Fig. 3i). Moreover, no significant erosion was observed in the epithelium of mouse cornea after topical administration of **3b** (Supplementary Fig. S14), indicating that **3b** was biocompatible to the corneal epithelium and underlying stroma. AmB has poor solubility in water and is unstable in aqueous, acidic or alkaline solution[21]. The water-soluble and stable antifungal compound **3b** is a better alternative to AmB.

Discussion

As fungi are metabolically similar to mammalian cells, limited fungi-specific targets are available for host differentiation. There is a pressing need to develop efficient and pathogen-specific antifungal agents to mitigate growing drug resistance problems. Our results show that a novel class of pathogen-specific, low-molecular weight antifungal agents have been successfully synthesized for self-assembly and therapeutic activity. These compounds have an exact molecular weight with a specific molecular recognition motif imparting polymer-like solid state properties—T_g and fibre-like assembly in water. The multivalent cationic charges of the self-assembled nanostructures facilitated lysis of fungal membranes with low MIC values and high selectivity. The cationic assemblies demonstrated efficient antifungal activity against clinically isolated drug-resistant strains, and effectively dispersed biofilms. In addition, they did not develop drug resistance after multiple sub-lethal treatments due to their membrane-lytic antifungal mechanism. Importantly, the nano-assemblies significantly decreased fungal counts, hindered hyphal corneal invasion and reduced the severity of keratitis in a fungal keratitis mouse model. They were also shown to have excellent *in vitro* and *in vivo* biocompatibility. Therefore, these small-molecule compounds hold great potential as antifungal agents for the prevention and treatment of topical fungus-induced infections where large and local doses can be administered.

Methods

PET degradation with 4-aminobenzylamine. PET flakes (9.61 g, 0.05 mol), 4-aminobenzylamine (28.2 g, 0.23 mol) and TBD (0.36 g, 2.5 mmol) were placed in a 250-ml flask, and then heated under nitrogen atmosphere at 120 °C for 3 h during which the reaction mixture solidified. The mixture was triturated and washed in isopropanol (200 ml). The residue was rinsed with THF and diethylether several times, and then dried in a vacuum oven at 80 °C, yielding a white powder as a product, bis(4-aminobenzyl)terephthalamide (4ABTA: 15.15 g, 81%). ^{1}H-NMR (400 MHz, dimethyl sulfoxide (DMSO)-d_6): δ 8.96 (*t*, $J=6$ Hz, 2H, N*H*), 7.93 (*s*, 4H, Ar-*H*), 6.98 (*d*, $J=8$ Hz, 4H, Ar-*H*), 6.51 (*d*, $J=8$ Hz, Ar-*H*), 4.96 (*s*, 4H, NH_2), 4.30 (*d*, $J=6$ Hz, 4H, CH_2). ^{13}C-NMR (100 MHz, DMSO-d_6): δ 165.4, 147.6, 136.7, 128.4, 127.3, 126.4, 113.8, 42.5. m.p. (DSC): 203 °C. The brief procedure for preparation of compound **3b** is given below as a typical example.

Synthesis of compound 3b. To a dry dimethylformamide (DMF) solution (16 ml) of pentafluorophenyl carbonate (PFC) (3.97 g, 10.1 mmol) was added a dry DMF solution (8 ml) of the diamine, N^1,N^4-bis(4-aminobenzyl)terephthalamide (4ABTA, **1**) (1.50 g, 4.0 mmol). The reaction mixture was stirred for 1 h at room temperature. Subsequently, *tert*-butyl (4-aminobutyl)carbamate (2.36 g, 12.6 mmol) was added, and the mixture was kept stirring overnight. To remove excess PFC and the amine reagent, the reaction mixture was precipitated in diethylether (250 ml). Thereafter, the product was filtered and dried in vacuum (60 °C) to yield **2b** (2.87 g, 90%). ^{1}H-NMR (400 MHz, DMSO-d_6): δ 9.08 (*t*, $J=5.8$ Hz, 2H, Ar-CON*H*), 8.36 (*s*, 2H, Ar-N*H*), 7.95 (*s*, 4H, Ar-*H*), 7.32 (*d*, $J=8.4$ Hz, 4H, Ar-*H*), 7.17 (*d*, $J=8.4$ Hz, 4H, Ar-*H*), 6.82 (*t*, $J=5.6$ Hz, 2H, N*H*COO), 6.07 (*t*, $J=5.6$ Hz, 2H, N*H*CH$_2$), 4.39 (*d*, $J=5.6$ Hz, 2H, Ar-C*H*$_2$), 3.09–3.00 (*m*, 4H, C*H*$_2$NHCOO), 2.95–2.86 (*m*, 4H, NHC*H*$_2$), 1.41–1.32 (*m*, 26H, C*H*$_2$ and C*H*$_3$). ^{13}C-NMR (100 MHz, DMSO-d_6): 165.3, 155.5, 155.1, 139.3, 136.6, 131.8, 127.7, 127.2, 117.4, 77.3, 42.2, 39.6, 38.7, 28.2, 27.2, 27.0.

The compound **2b** (2.50 g, 3.11 mmol) was added into trifluoroacetic acid (TFA, 10 ml) and the mixture was stirred overnight. As the deprotection proceeded, the reaction mixture became homogeneous. The reaction mixture was then precipitated in diethylether (200 ml), and the precipitate was filtered and washed with diethylether a few times, and dried in vacuum (60 °C) to yield **3b** (2.07 g, 80%). ^{1}H-NMR (400 MHz, DMSO-d_6): δ 9.09 (*t*, $J=5.8$ Hz, 2H, Ar-CON*H*), 8.56 (*s*, 2H, Ar-N*H*), 7.95 (*s*, 4H, Ar-*H*), 7.72 (*b*, 6H, NH_3^+), 7.34 (*d*, $J=8.4$ Hz, 4H, Ar-*H*), 7.17 (*d*, $J=8.4$ Hz, 4H, Ar-*H*), 6.30 (*t*, $J=5.8$ Hz, 2H, N*H*CH$_2$), 4.39 (*d*, $J=5.6$ Hz, 2H, Ar-C*H*$_2$), 3.08 (*ddd*, $J=6.2$, 6.2, 6.0 Hz, 4H, C*H*$_2$NH), 2.80 (*t*, $J=7.4$ Hz, 4H, C*H*$_3$), 1.59–1.39 (*m*, 8H, C*H*$_2$). ^{13}C-NMR (100 MHz, DMSO-d_6): 165.3, 158.4, 155.3, 139.4, 136.6, 131.8, 127.7, 127.2, 117.5, 74.7(*t*), 42.2, 38.6, 38.3, 26.8, 24.4.

***In vitro* antifungal assays.** The MICs of the cationic compounds were measured using a broth microdilution method[22]. First, cationic compounds were dissolved in de-ionized (DI) water at 2,500 mg l^{-1}. The samples were further diluted to 31.25, 62.5, 125.0, 250.0, 500.0 and 1,000 mg l^{-1}. *C. albicans* and *C. neoformans* were grown in yeast mould broth (YMB) and Mueller Hinton broth (MHB), respectively, with vigorous shaking, and they were cultured at room temperature and 37 °C, respectively. The optical density ($OD_{600\,nm}$) of the fungus solution was adjusted to 0.1 by the addition of YMB or MHB. This fungus solution was further diluted to 10^5 CFU ml^{-1} using YMB or MHB. Cationic compound solution (100 µl) was transferred to each well of a 96-well plate (NUNC), followed by the addition of 100 µl of the fungus solution. YMB and MHB were used as the control. The optical density readings of fungus solutions were monitored by measuring $OD_{600\,nm}$ at predetermined times (0 h and 24 h) using a microplate reader (TECAN). The assay was performed in four replicates for each sample and the experiments were repeated at least three times.

Antifungal activities of cationic compounds were further tested through a spread plate method. Briefly, *C. albicans* and *C. neoformans* were treated at specific concentrations of cationic compounds. At predetermined time points, microbial suspensions (20 or 100 µl) were withdrawn and diluted sequentially and then plated on 1.5% LB agar plates. The plates were incubated for 48 h at room temperature. Microbial colonies were formed and counted. The results were expressed as mean $\log_{10}$ (CFU ml^{-1}). The experiments were performed in triplicates, and were repeated three times.

Drug resistance studies. *C. albicans* was used as a model microbe for drug resistance studies. Drug resistance was induced by treating the *C. albicans* repeatedly with antimicrobial agents[23]. The MIC of **3b** against *C. albicans* was tested for 11 passages of growth. MIC was determined using the broth microdilution method. *C. albicans* exposed to the sub-MIC concentration (1/8 of MIC at that particular passage) were re-grown to a logarithmic growth phrase, and re-used for the subsequent passage's MIC measurement for the same antimicrobial agent. Drug-resistant behaviour of *C. albicans* was evaluated by recording the changes in the MIC normalized to that of the first passage. Conventional antifungal agent fluconazole was used as the control.

Haemolysis assay. Fresh rat blood cells were diluted with PBS buffer to give a cell suspension (4% in volume). Cell suspension (100 µl) was introduced to each well of a 96-well plate, and 100 µl of cationic compound solution was then added to the well. PBS and Triton X-100 (0.2%) were used as the control. The plates were incubated for 1 h at 37 °C. The 96-well plates were centrifuged at 2,200 r.p.m. for 5 min. Aliquots (100 µl) of the supernatant were transferred to a new 96-well plate. Haemoglobin release was measured at 576 nm using a microplate reader (TECAN). The red blood cells in PBS were used as a negative control. Absorbance of wells with red blood cells lysed with 0.2% Triton X-100 was taken as 100% haemolysis. Percentage of haemolysis was calculated using the following formula: haemolysis (%) = [(OD_{576nm} in the sample − OD_{576nm} in PBS)/(OD_{576nm} in 0.2% Triton X-100 − OD_{576nm} in PBS)] × 100. The data were expressed as mean and s.d. of four replicates, and the tests were repeated three times.

MTT assay. The cytotoxicity tests of cationic compounds were performed in human dermal fibroblasts using MTT assay. The cells were cultured in Dulbecco's Modified Eagle Medium (DMEM) supplemented with 10% FBS, 5% penicillin, 2 mM L-glutamine (Sigma) and incubated at 37 °C in 5% CO_2. The cells were seeded onto 96-well plates at a density of 10,000 cells per well and incubated for 1 day. Cationic compounds were diluted with the growth medium to give final concentrations of 31.25, 62.50, 125.0, 250.0, 500.0 and 1,000 mg l^{-1}. The media were replaced with 100 µl of the pre-prepared samples. The plates were then returned to the incubator and maintained in 5% CO_2 at 37 °C for 24 h. Fresh growth media (100 µl) containing 10% MTT solution (5 mg ml^{-1}) were used to replace the mixture in each well after 24 h. The plates were then returned to the incubator, and maintained in 5% CO_2 at 37 °C for another 4 h. The growth medium and excess MTT in each well were then removed. DMSO (150 µl) was then added to each well to dissolve the internalized purple formazan crystals. An aliquot of 100 µl was taken from each well, and transferred to a new 96-well plate. Each sample was tested in eight replicates per plate. The plates were then assayed at 550 nm and 690 nm. The absorbance readings of the formazan crystals were taken to be that at 550 nm subtracted by that at 690 nm. The results were expressed as a percentage of the absorbance of the blank control.

SEM analysis. The *C. albicans* before and after incubation with cationic compound **3b** at MIC for 2 h were harvested by centrifugation at 4,000 r.p.m. for 5 min. They were washed by PBS three times, and then fixed in formalin solution containing 4% formaldehyde overnight. The cells were further washed with DI water, followed by dehydration using a series of ethanol solutions with different volume contents (35, 50, 75, 90, 95 and 100%). The sample was placed on a carbon tape, which was further coated with platinum. The morphologies of the *C. albicans* before and after the treatment were observed using a field emission scanning electron microscope (JEOL JSM-7400F) operated at an accelerating voltage of 10.0 kV and a working distance of 8.0 mm.

TEM analysis. The morphologies of the cationic compounds were analysed by TEM (FEI Tecnai G^2 F20 electron microscope). Samples were prepared by a membrane dialysis method. The cationic compounds (10 mg) were dissolved in

2 ml of DMF. The solution was then dialyzed against DI water at 20 °C for 24 h using a dialysis membrane with a molecular weight cutoff of 1,000 (Spectra/Por 7, Spectrum Laboratories Inc.). Cationic compounds solution (5 µl) was placed on a copper grid coated with carbon film and incubated for 1 min. Phosphotungstic acid (5 µl; 0.1 w/v%) was applied and incubated for another minute. The extra sample solution on the grid was absorbed by filter paper. The samples were air-dried at room temperature. The TEM studies were conducted with an electron kinetic energy of 200 keV.

The morphologies of the *C. neoformans* before and after treatment with cationic compound **3b** were observed under a JEM-1230 transmission electron microscope (JEOL, Japan) using an acceleration voltage of 80 keV. The *C. neoformans* (1.5 ml) were incubated with 0.5 ml of **3b** solution at 2 × MIC for 8 h. The solution was then centrifuged at 4,000 r.p.m. for 10 min, and the supernatants were removed. They were washed by PBS (pH 7.0) twice, and then fixed in formalin solution containing 2.5% glutaraldehyde overnight. The samples were then washed by PBS three times (15 min each), and post-fixed with 1% OsO_4 in the phosphate buffer (pH 7.0) for 1 h. The fixed samples were washed in the phosphate buffer three times (15 min each), followed by dehydration in a graded ethanol solution series. The samples were incubated with a mixture of acetone and Spurr resin (1:1 in volume) for 1 h at room temperature, and then transferred to a 1:3 mixture of acetone and Spurr resin for 3 h, and lastly to Spurr resin for overnight incubation. Ultrathin sections (70–90 nm) were obtained with a Reichert–Jung Ultracut E ultramicrotome, and post-stained with uranyl acetate and lead citrate for 15 min each prior to the TEM studies.

Membrane integrity test. To further elucidate that the fungal membrane was damaged after the treatment, the presence of 260 nm-absorbing molecules in the culture media was tested after 3 h of incubation with the nanostructures according to a previously reported protocol[18]. Briefly, overnight culture of *C. albicans* was first adjusted to contain 3×10^6 CFU ml^{-1} with sterile PBS. Antifungal solutions were prepared at different concentrations of **3b** by serial dilutions with sterile DI water. Equal volumes of fungal suspension and antifungal solution were then mixed to achieve the final **3b** concentrations ranging from MIC to 4 × MIC, and the mixture was incubated for 3 h. The microbial suspension was filtered with 0.22-mm filter to remove the fungal cells from the suspension, and the absorbance of the filtrate solution was measured at 260 nm using a ultraviolet-visible spectrophotometer (Nanodrop ND-1000, Biofrontiers Technology, Singapore). The experiment was performed in triplicate, and untreated fungal suspension was used as the negative control to normalize the absorbance reading of the experimental groups.

Biofilm formation. *C. albicans* biofilm was formed on contact lenses (Air optix, CIBA Vision). The contact lens was cut into pieces of 2 mm in diameter and transferred into a six-well plate. The samples were soaked in YMB overnight at 37 °C. Broth solution was withdrawn from the plates, followed by addition of 4 ml of *C. albicans* (10^7 CFU ml^{-1}) to each well. The plates were incubated at room temperature with shaking at 100 r.p.m. After 5 h of incubation, suspension was withdrawn and the lenses were washed by phosphate buffered saline (PBS) (pH 7.4) to remove any non-adherent cells, followed by the addition of 4 ml of fresh YMB. The plates containing the contact lenses with cells adhered were incubated at room temperature with shaking at 100 r.p.m. for 2 days to allow biofilm formation.

***In vitro* anti-biofilm assays.** Contact lenses containing biofilms were transferred to individual wells of a new 24-well plate. Biofilms were washed three times using PBS (pH 7.4) to remove non-adhered cells. Solution (500 µl) containing different concentrations of **3b** was added to each well containing biofilm, which was incubated for another day. Blank contact lenses were used as the control. After treatment, the solution was withdrawn from each well, and the biofilm was washed with PBS. The viability of cells in the biofilm was determined by XTT assay. This assay is based on the reduction of XTT tetrazolium salt to XTT formazan by mitochondrial dehydrogenases. Briefly, 200 µl of PBS containing 20 µl of XTT solution (1 mg ml^{-1}) and 4 µl of menadione solution (1 mM) were added to each well. Plates were then incubated at 37 °C for 3 h. The colorimetric change associated with cell viability was measured using the microplate reader at 490 nm. The results were expressed as a percentage of the absorbance of the untreated samples.

The ECM production was quantified by Safranin assay. Briefly, the biofilms were stained with 200 µl of aqueous solution containing 0.1% Safranin O for 15 min. The excess stain was removed by washing with PBS. The stained biofilm was solubilized with 200 µl of 70% ethanol for 15 min and the optical absorbance at 550 nm was recorded using the microplate reader. The assay was performed in four replicates for each sample, and the experiments were repeated at least three times. The readings were normalized to that of the untreated samples.

The biofilm samples before and after **3b** treatment (500 mg l^{-1}) for SEM images were prepared using a similar method as described earlier. The biofilms formed on contact lenses were also observed with confocal laser scanning fluorescence microscopy (CLSM). Briefly, contact lenses containing biofilms before and after **3b** treatment at 500 mg l^{-1} were washed three times using PBS, and transferred to individual wells of a new 24-well plate. The samples were stained with 1 ml of PBS solution containing 25 mg l^{-1} of green fluorescence CON-A (excitation wavelength: 488 nm; emission wavelength: 505 nm) and 10 µM of red fluorescence FUN-1 (excitation wavelength: 543 nm; emission wavelength: 560 nm) for 30 min at 37 °C, followed by rinsing with PBS solution. Samples were visualized by Carl Zeiss LSM 510 META confocal microscope (Germany). Three-dimensional (3D) reconstruction of images was obtained with Imaris software. All images were obtained under the same conditions.

***In vivo* toxicity evaluation.** C57BL/6 mice (8 weeks old, 18–22 g) were used for animal studies. The mice were randomly grouped. In each group, a total of three mice were used. The compound **3b** (2,000 mg l^{-1} in aqueous solution) was administered to the eyes every 5 min during the first hour and every 30 min during the next 7 h. All mice were killed after the administration of the last eye drop. The treated eyeballs were collected and fixed in 4% neutral buffered formalin. The fixed eyeballs were embedded in paraffin, sectioned and stained with hematoxylin (nucleus, blue) and eosin (cytoplasma, purple) by the standard protocol. The eyeballs treated with water were used as control.

Keratitis model. Keratitis model was established by a previously reported method[19,20]. The mice were immune suppressed via subcutaneously injecting cyclophosphamide (Sigma-Aldrich, 180 g per kg) at 5 days, 3 days and 1 day before inducing keratitis. The mice were anaesthetized by ketamine (150 mg per kg) and xylazine (10 mg ml^{-1}) by intraperitoneal injection. Additional corneal anaesthesia was also performed with 0.5% tetracaine hydrochloride eye drops (Bausch & Lomb, Tampa, Florida). A 2-mm filter paper disc moistened with 99% 1-heptanol (Sigma-Aldrich, Lausanne, Switzerland) was placed on the centre of the cornea for 40 s. The corneal epithelium was wiped off and the eyes were rinsed with PBS removing any remaining 1-heptanol. A 2 mm-diameter punch from the contact lens with *C. albicans* biofilm was then placed on the denuded cornea surface. The lids were closed with silk sutures to keep the contact lenses inside. Eye ulcer with a leathery, tough and raised surface was observed after *C. albicans* were introduced on the eyeball for 18 h. The eye lids were then opened and the lens was removed. The mice with keratitis were randomly grouped in groups of nine and treated with three topical eye drop solutions: water (control), 2,000 mg l^{-1} of **3b** and 1,500 mg l^{-1} of amphotericin B (AmB, Sigma-Aldrich, Lausanne, Switzerland). AmB was used as positive control. Eye drops (20 µl each) were administered to the mice every 5 min during the first hour and every 30 min during the next 7 h. The severity of keratitis was graded in clinical scores ranging from 1 to 12 based on the scoring system reported by Wu *et al.*[20] to evaluate treatment efficacy. A disease grading of 1–4 was assigned to the area of opacity, density of opacity and surface regularity (Supplementary Table S2). A total score of ≤ 5, 6–9 and >9 indicate mild, moderate and severe keratitis, respectively.

All mice were killed after the administration of the last eye drop. The treated eyeballs were collected immediately; three eyeballs from each group were collected for histology, and the remaining six eyeballs were homogenized (Pro200 tissue homogenizer) for quantitative analysis of fungal counts. Briefly, aliquots of serial dilutions were plated in triplicate on agar plates, and the plates were incubated for 48 h at room temperature before the colonies were counted. The number of CFUs recovered was expressed as mean $\log_{10}$ CFU per eye. The fixed eyeballs were embedded in paraffin, sectioned and stained with Grocott's methenamine silver or periodic acid-Schiff reagent by the standard protocol for histological analysis. To determine the extent of hyphal invasion into corneal stroma, each stained section obtained from cornea was imaged using a light microscope (Olympus, Japan). Three representative images per group with a total of 150 points (50 points for each image) were analysed for the absolute deepest depth of corneal penetration at each point using AutoCAD software.

Statistics analysis. The data were expressed as mean ± s.d. (s.d. is indicated by the error bars). Student's *t*-test was used to determine significance among groups. A value of $P<0.05$ was considered to be significant.

References

1. Ostrosky-Zeichner, L., Casadevall, A., Galgiani, J. N., Odds, F. C. & Rex, J. H. An insight into the antifungal pipeline: selected new molecules and beyond. *Nat. Rev. Drug Discov.* **9,** 719–727 (2010).
2. Berman, J. & Sudbery, P. E. Candida albicans: a molecular revolution built on lessons from budding yeast. *Nat. Rev. Genet.* **3,** 918–930 (2002).
3. Wisplinghoff, H. *et al.* Nosocomial bloodstream infections in US hospitals: analysis of 24,179 cases from a prospective nationwide surveillance study. *Clin. Infect. Dis.* **39,** 309–317 (2004).
4. Anderson, J. B. Evolution of antifungal-drug resistance: Mechanisms and pathogen fitness. *Nat. Rev. Microbiol.* **3,** 547–556 (2005).
5. Cowen, L. E. The evolution of fungal drug resistance: modulating the trajectory from genotype to phenotype. *Nat. Rev. Microbiol.* **6,** 187–198 (2008).
6. Hartsel, S. & Bolard, J. Amphotericin B: new life for an old drug. *Trends Pharmacol. Sci.* **17,** 445–449 (1996).
7. Fanos, V. & Cataldi, L. Amphotericin B-induced nephrotoxicity: a review. *J. Chemother.* **12,** 463–470 (2000).

8. Brogden, K. A. Antimicrobial peptides: pore formers or metabolic inhibitors in bacteria? *Nat. Rev. Microbiol.* **3,** 238–250 (2005).
9. Nederberg, F. *et al.* Biodegradable nanostructures with selective lysis of microbial membranes. *Nat. Chem.* **3,** 409–414 (2011).
10. Liu, L. H. *et al.* Self-assembled cationic peptide nanoparticles as an efficient antimicrobial agent. *Nat. Nanotech.* **4,** 457–463 (2009).
11. Qiao, Y. *et al.* Highly dynamic biodegradable micelles capable of lysing Gram-positive and Gram-negative bacterial membrane. *Biomaterials* **33,** 1146–1153 (2011).
12. Silva, A. D. *et al.* A fundamental study on dissolution behavior of high-resolution molecular glass photoresists. *Chem. Mater.* **20,** 7292–7300 (2008).
13. Klepser, M. E., Ernst, E. J., Lewis, R. E., Ernst, M. E. & Pfaller, M. A. Influence of test conditions on antifungal time-kill curve results: proposal for standardized methods. *Antimicrob. Agents Chemother.* **42,** 1207–1212 (1998).
14. Rex, J. H. *et al.* Development of interpretive breakpoints for antifungal susceptibility testing: conceptual framework and analysis of *in vitro in vivo* correlation data for fluconazole, itraconazole, and Candida infections. *Clin. Infect. Dis.* **24,** 235–247 (1997).
15. Douglas, L. J. Candida biofilms and their role in infection. *Trends Microbiol.* **11,** 30–36 (2003).
16. Finkel, J. S. & Mitchell, A. P. Genetic control of *Candida albicans* biofilm development. *Nat. Rev. Microbiol.* **9,** 109–118 (2011).
17. Chandra, J., Mukherjee, P. K. & Ghannoum, M. A. *In vitro* growth and analysis of Candida biofilms. *Nat. Protoc.* **3,** 1909–1924 (2008).
18. Chen, C. Z. & Cooper, S. L. Interactions between dendrimer biocides and bacterial membranes. *Biomaterials* **23,** 3359–3368 (2002).
19. Goldblum, D., Frueh, B. E., Sarra, G. M., Katsoulis, K. & Zimmerli, S. Topical caspofungin for treatment of keratitis caused by *Candida albicans* in a rabbit model. *Antimicrob. Agents Chemother.* **49,** 1359–1363 (2005).
20. Wu, T. G., Wilhelmus, K. R. & Mitchell, B. M. Experimental keratomycosis in a mouse model. *Invest. Ophthalmol. Vis. Sci.* **44,** 210–216 (2003).
21. Keay, L. *et al.* Microbial keratitis: Predisposing factors and morbidity. *Ophthalmology* **113,** 109–116 (2006).
22. Wiegand, I., Hilpert, K. & Hancock, R. E. W. Agar and broth dilution methods to determine the minimal inhibitory concentration (MIC) of antimicrobial substances. *Nat. Protoc.* **3,** 163–175 (2008).
23. Dzidic, S., Suskovic, J. & Kos, B. Antibiotic resistance mechanisms in bacteria: biochemical and genetic aspects. *Food Technol. Biotechnol.* **46,** 11–21 (2008).

Acknowledgements

We would like to acknowledge the financial support from IBM Almaden Research Center, USA, and the Institute of Bioengineering and Nanotechnology (Biomedical Research Council, A*STAR, Singapore).

Author contributions

J.L.H. and Y.Y.Y. oversaw the project and project planning. J.L.H. and K.F. synthesized the compounds. S.L. performed compound characterization and biological studies. H.W. and S.L. conducted the animal study, which was supervised by J.Y.Y. A.C.E. and D.J.C. contributed to DSC analysis. H.M. conducted AFM analysis. J.P. contributed to the computational modelling. N.W. studied the release of *C.* albicans cytoplasmic contents. S.V. performed TEM analysis of the compounds. Y.H. and W.F. contributed to MIC and killing efficiency against *C. neoformans* and TEM of *C. neoformans*. All the authors contributed to the paper writing.

Additional information

Supplementary Information accompanies this paper at http://www.nature.com/naturecommunications

Competing financial interests: The authors declare no competing financial interests.

Reprints and permission information is available online at http://npg.nature.com/reprintsandpermissions/

How to cite this article: Fukushima, K. *et al.* Supramolecular high-aspect ratio assemblies with strong antifungal activity. *Nat. Commun.* 4:2861 doi: 10.1038/ncomms3861 (2013).